

Supplementary information for

**Nanostructured robust cobalt metal alloy based anode electro-catalysts exhibiting
remarkably high performance and durability for proton exchange membrane fuel cells**

Prasad Prakash Patel¹, Moni Kanchan Datta^{2,3}, Oleg I. Velikhokhatnyi^{2,3}, Prashanth Jampani²,
Daeho Hong², James A. Poston⁴, Ayyakkannu Manivannan⁴, Prashant N. Kumta^{1,2,3,5,6*}

¹Department of Chemical and Petroleum Engineering, Swanson School of Engineering, University of Pittsburgh, Pittsburgh, PA 15261, USA.

²Department of Bioengineering, Swanson School of Engineering, University of Pittsburgh, Pittsburgh, PA 15261, USA.

³Center for Complex Engineered Multifunctional Materials, University of Pittsburgh, PA 15261, USA.

⁴US Department of Energy, National Energy Technology Laboratory, Morgantown, WV 26507.

⁵Mechanical Engineering and Materials Science, Swanson School of Engineering, University of Pittsburgh, Pittsburgh, PA 15261, USA.

⁶School of Dental Medicine, University of Pittsburgh, PA 15217, USA.

*Corresponding author: Prashant N. Kumta (pkumta@pitt.edu) Department of Bioengineering, 815C Benedum Hall, 3700 O'Hara Street, Pittsburgh, PA 15261.

Tel: +1-412-648-0223, Fax: +1-412-624-3699

This is an abstract presented at the 225th Electrochemical Society Meeting in Orlando, FL (May 11-15, 2014).

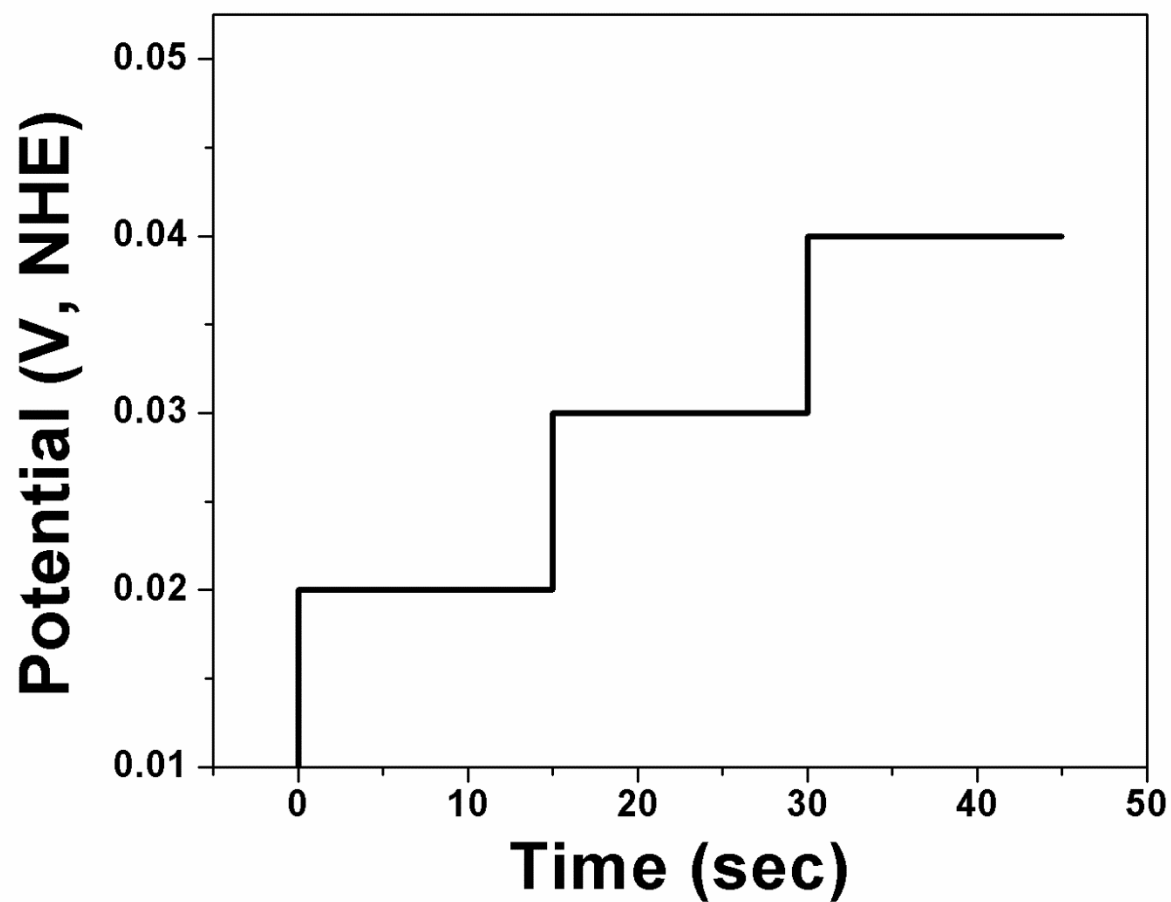


Figure S1: Method of multiple small potential steps used on the RDE to reduce the contribution by charging current and current measurement that was performed at the end of each step.

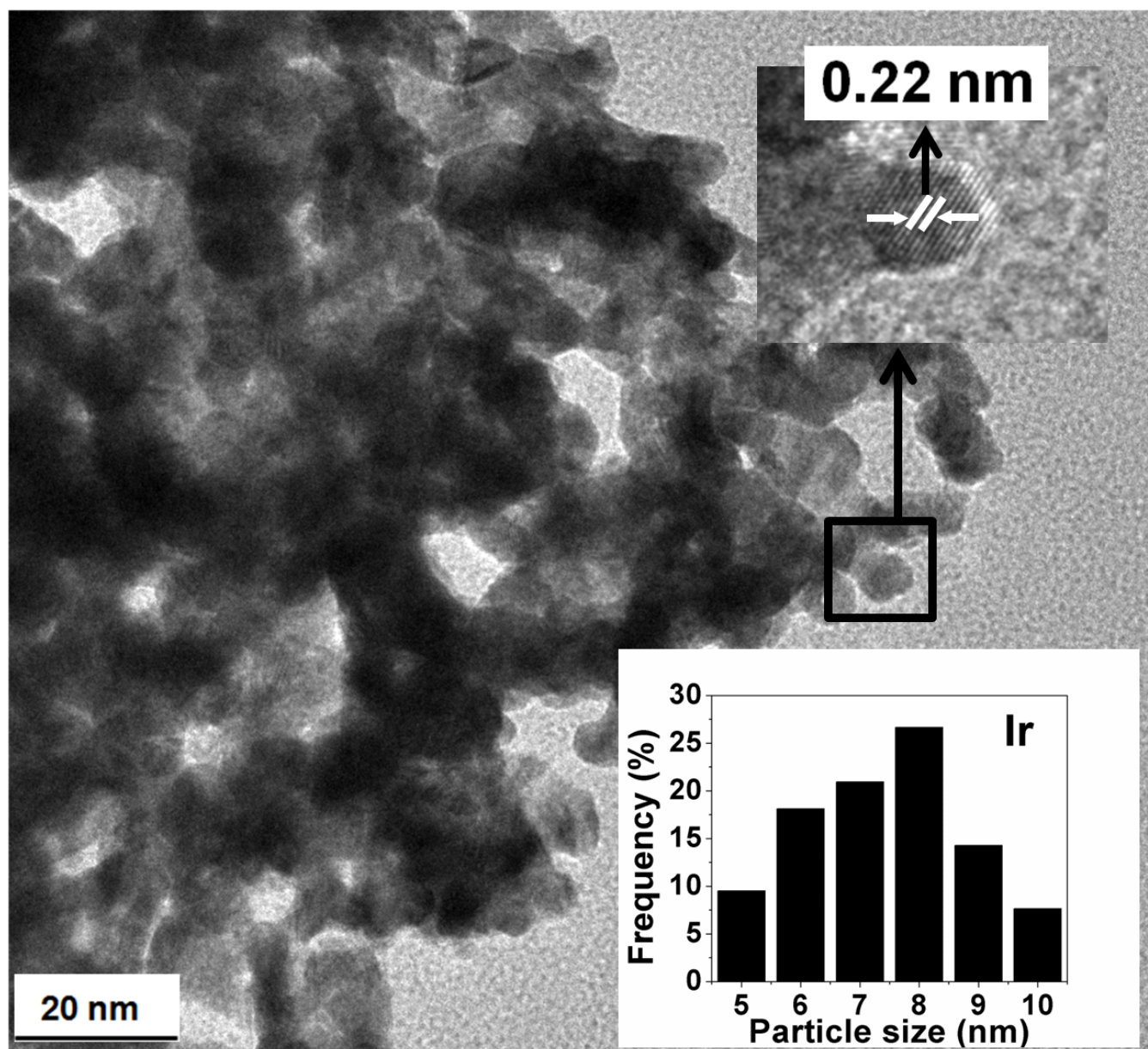


Figure S2: The bright field TEM image of Ir NPs showing the presence of fine nanoparticles with HRTEM image showing lattice fringes with a spacing of ~ 0.22 nm.

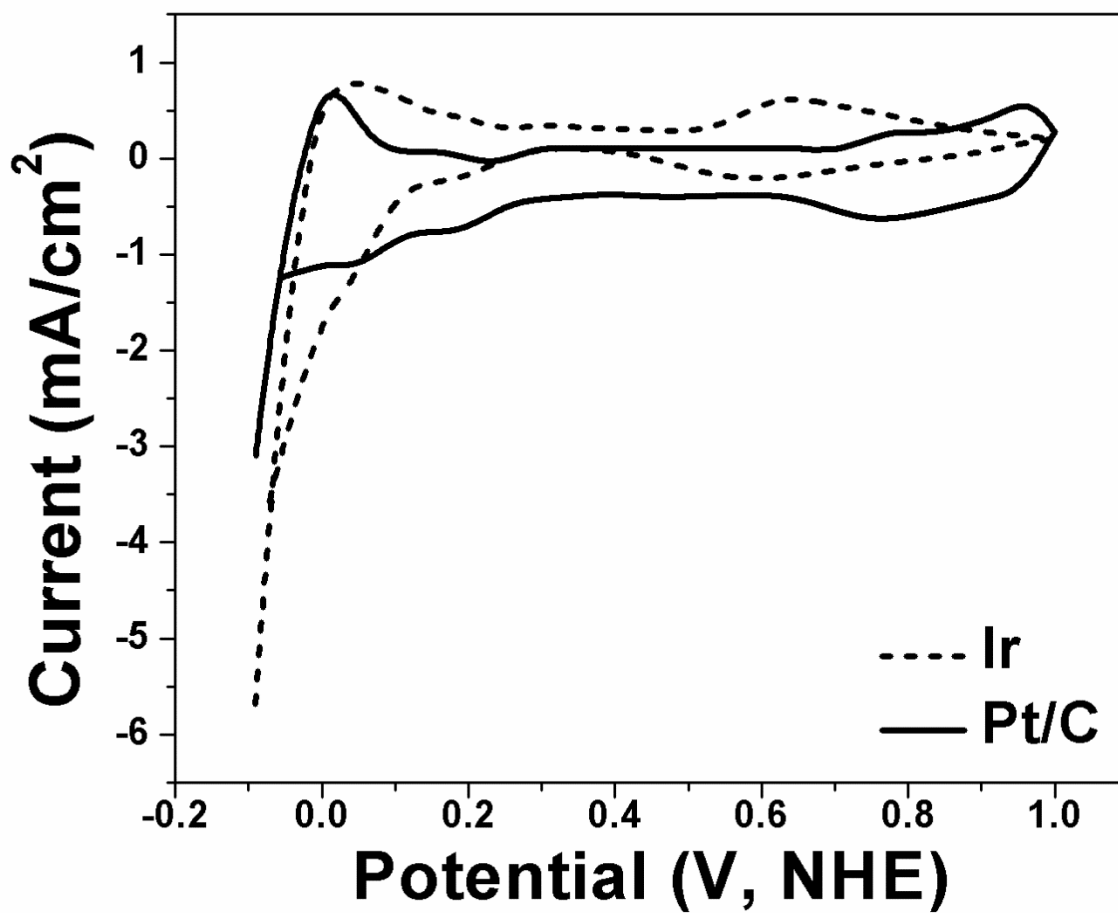


Figure S3: The cyclic voltammetry (CV) curve for HOR of Ir-NPs and Pt/C, measured in H₂ saturated 0.5 M H₂SO₄ electrolyte solution at 40°C at scan rate of 10 mV/sec.

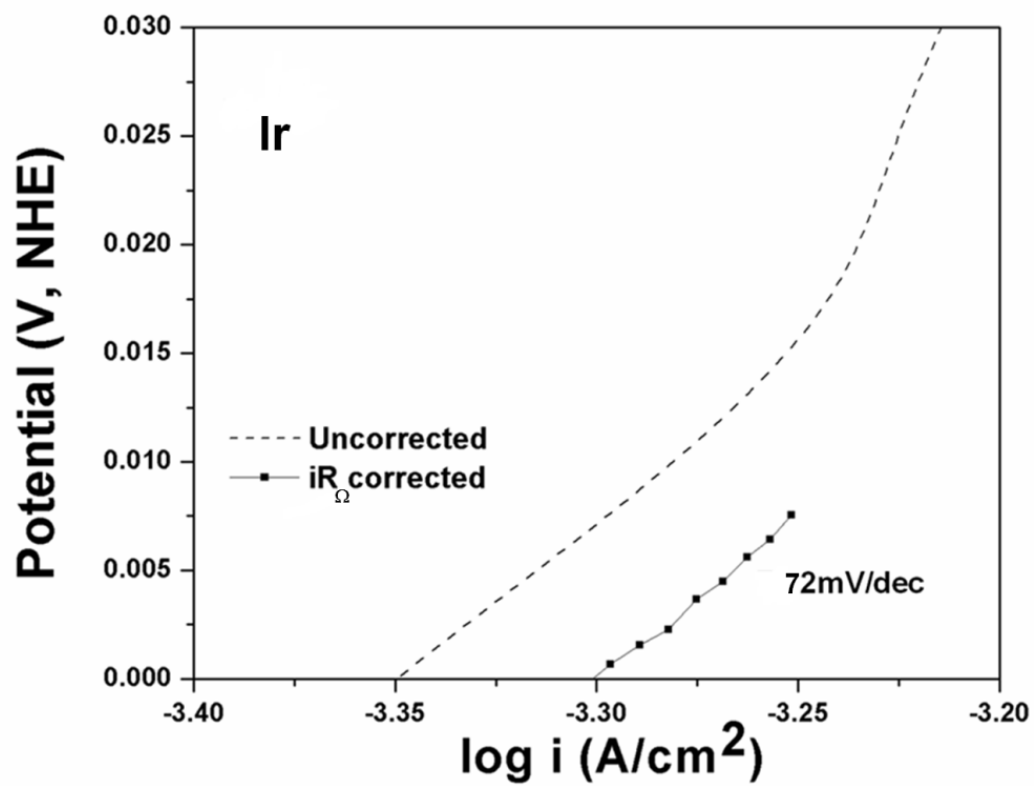


Figure S4: Tafel polarization plot of Ir NPs, before and after iR_{Ω} correction.

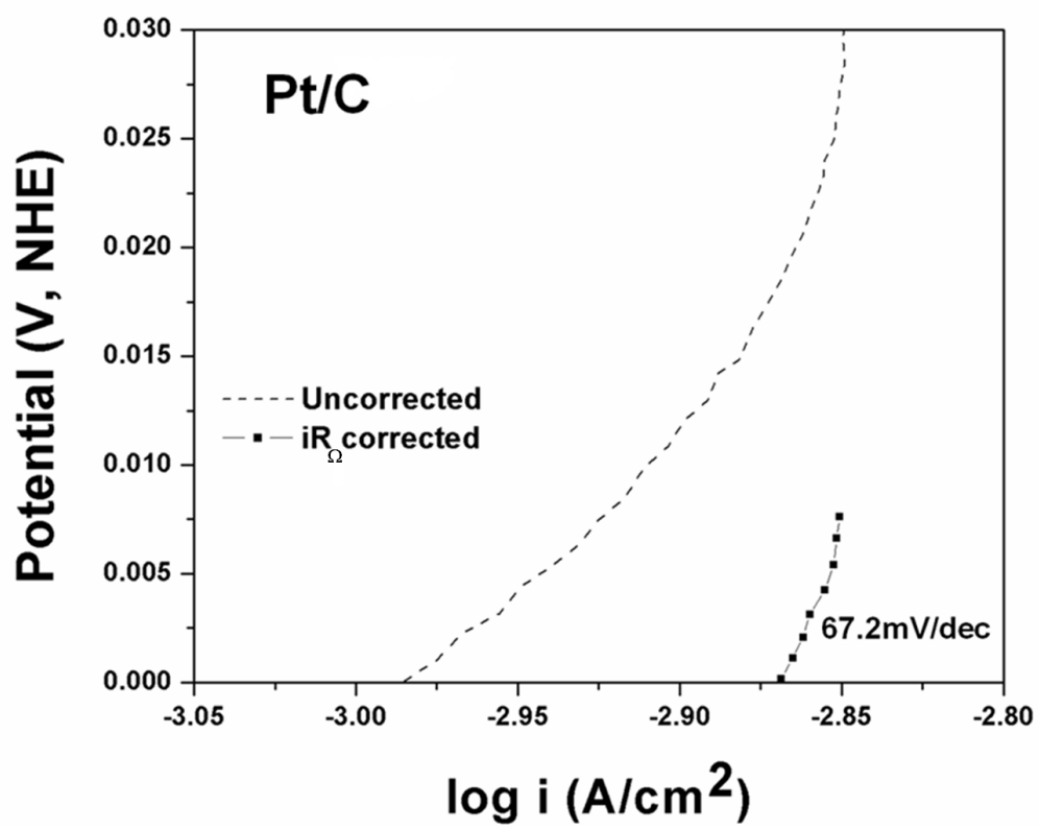


Figure S5: Tafel polarization plot of Pt/C, before and after iR_{Ω} correction.

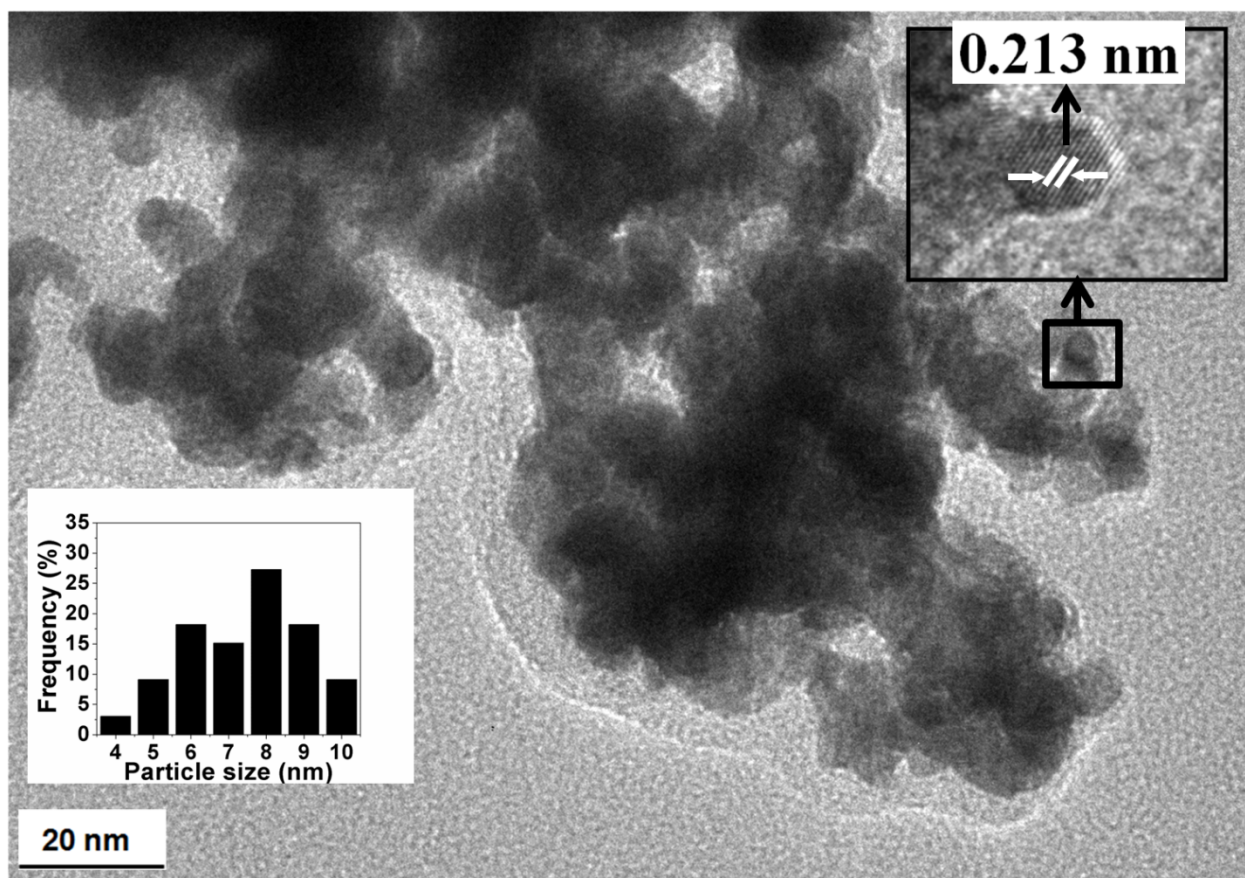
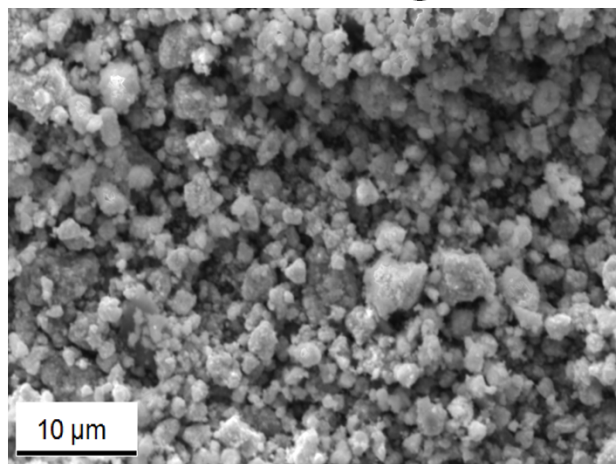
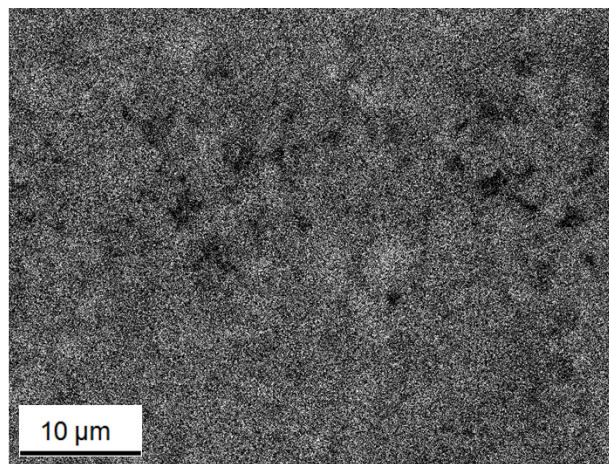


Figure S6: The bright field TEM image of $\text{Co}_{0.7}(\text{Ir}_{0.3})$ showing the presence of fine nanoparticles and the particle size distribution with the HRTEM inset image showing lattice fringes with a spacing of ~ 0.213 nm.

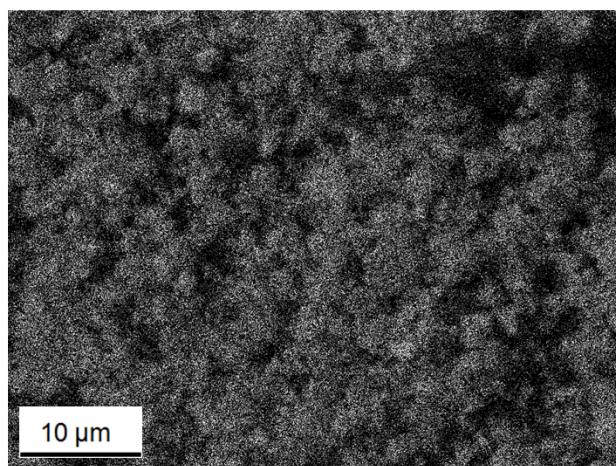
SEM Micrograph



Co



Ir



EDAX spectrum

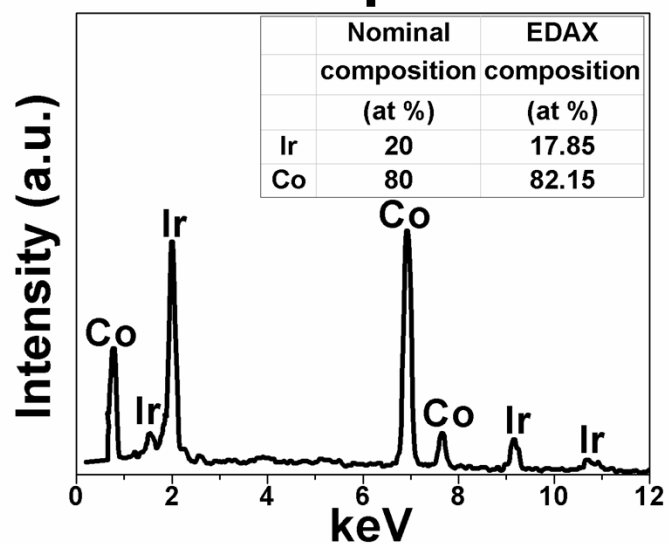
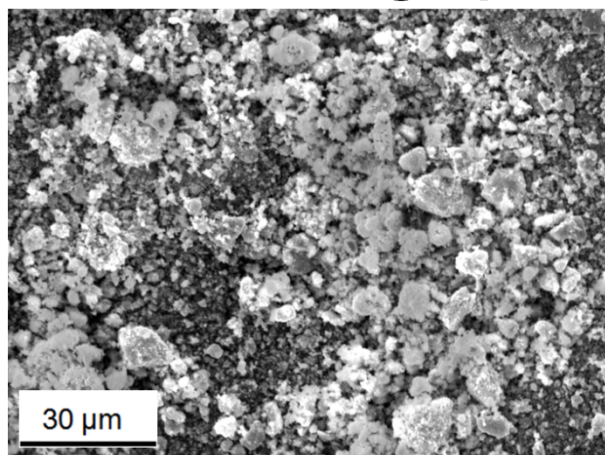
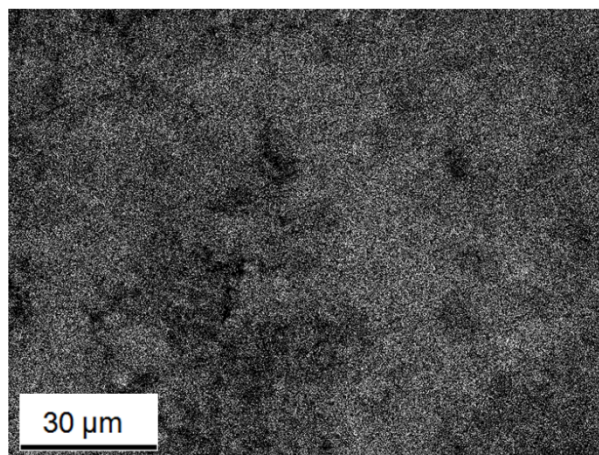


Figure S7: SEM micrograph and the corresponding elemental mapping, and EDAX spectrum of $\text{Co}_{0.8}(\text{Ir}_{0.2})$ collected from the solid solution nanoparticles.

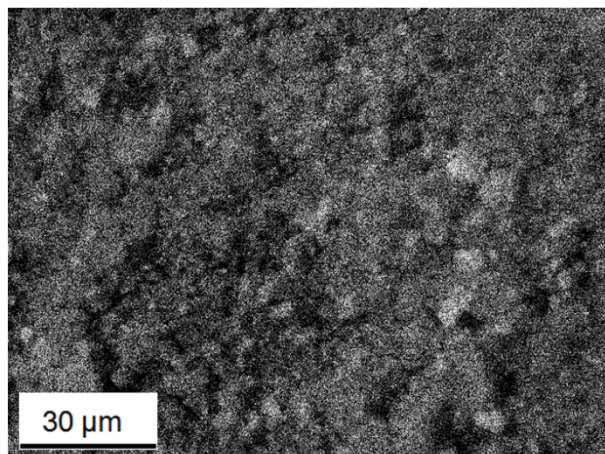
SEM Micrograph



Co



Ir



EDAX spectrum

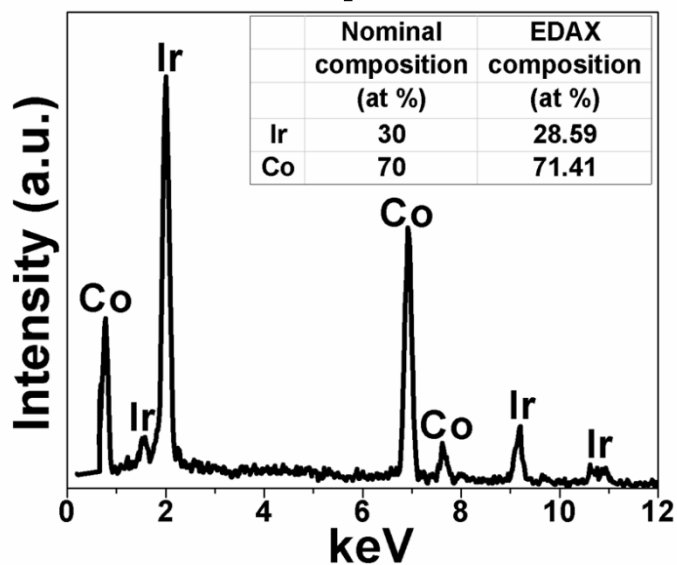
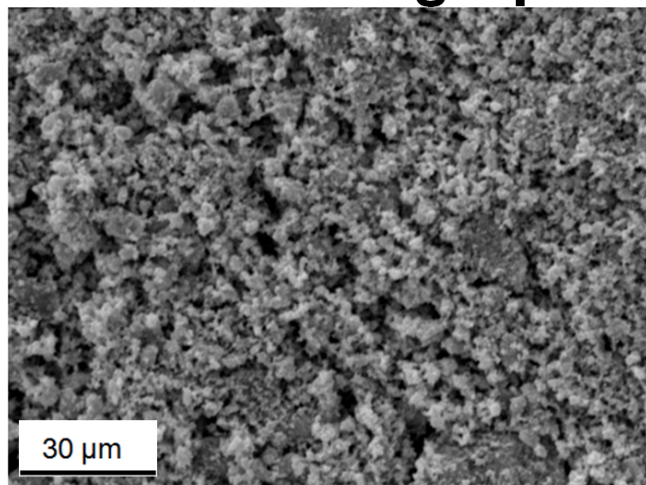
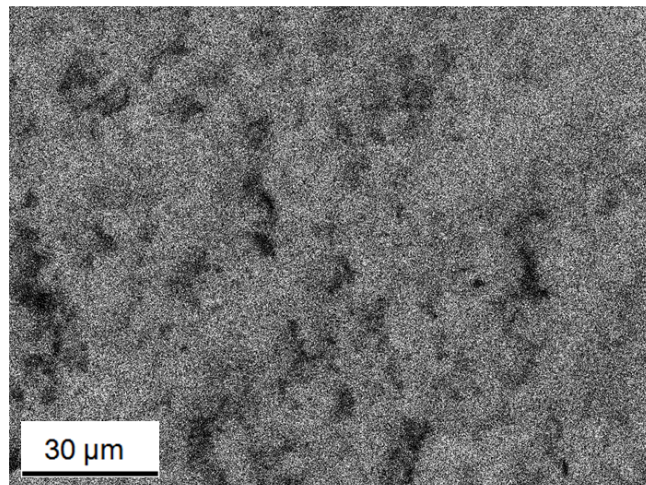


Figure S8: SEM micrograph and the corresponding elemental map and EDAX spectrum of $\text{Co}_{0.7}(\text{Ir}_{0.3})$ collected from the solid solution alloy nanoparticles.

SEM Micrograph



Ir



EDAX spectrum

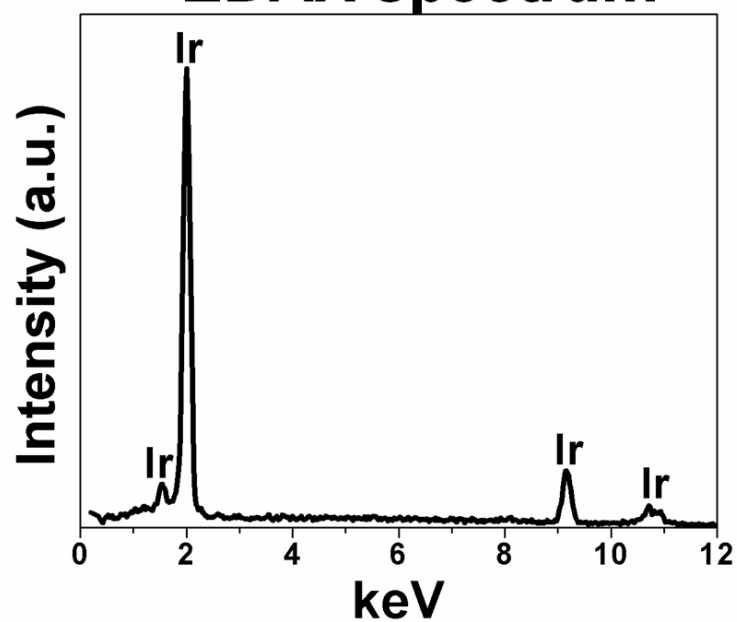


Figure S9: SEM micrograph and the corresponding elemental map and EDAX spectrum of Ir collected from the Ir nanoparticles.

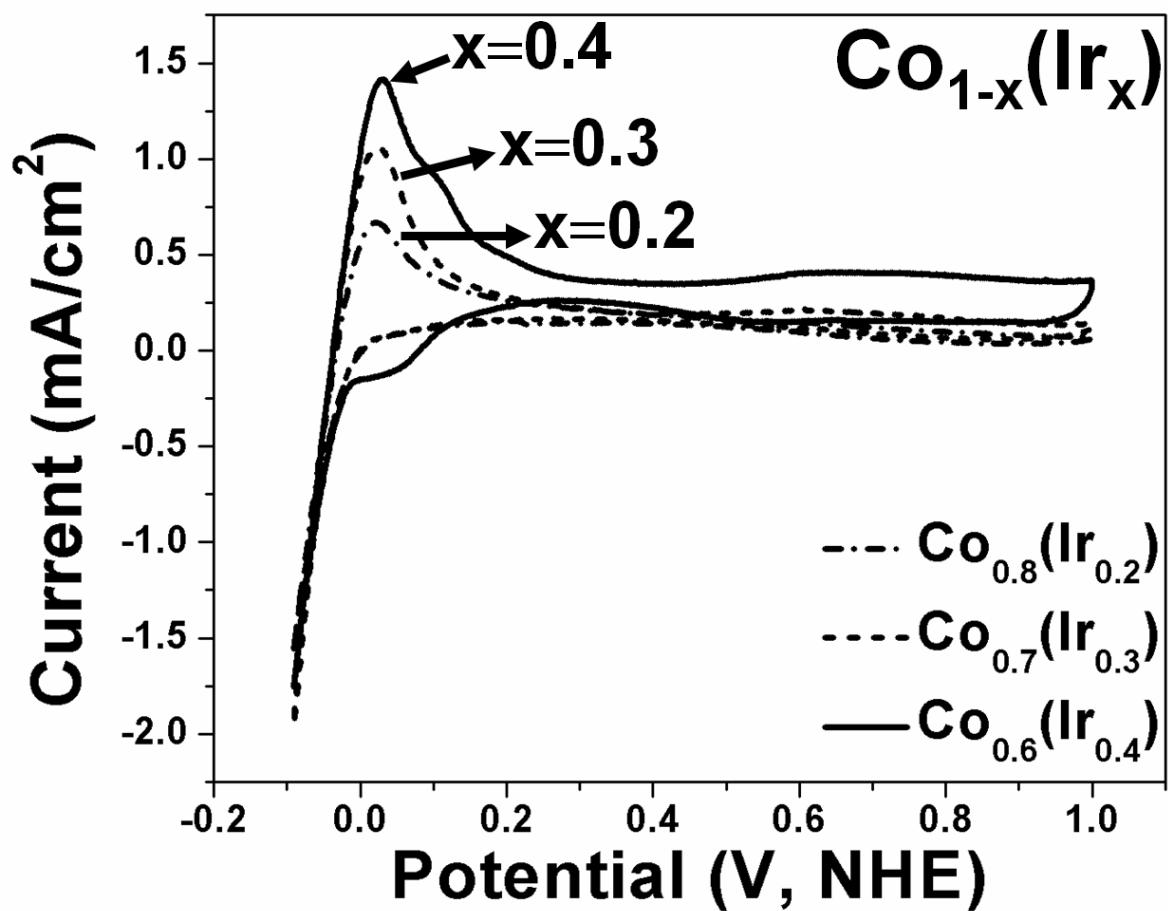


Figure S10: The cyclic voltammetry (CV) curve for HOR of $\text{Co}_{1-x}(\text{Ir}_x)$ ($x=0.2, 0.3, 0.4$), measured in H_2 saturated 0.5 M H_2SO_4 electrolyte solution at 40°C at scan rate of 10 mV/sec

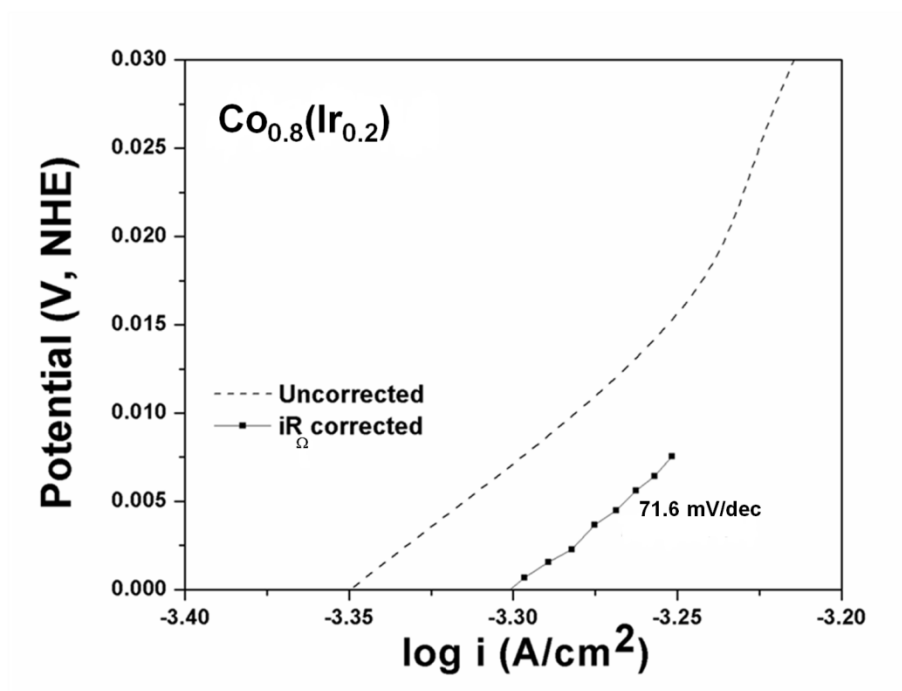


Figure S11: Tafel polarization plot of $\text{Co}_{0.8}(\text{Ir}_{0.2})$, before and after iR_{Ω} correction.

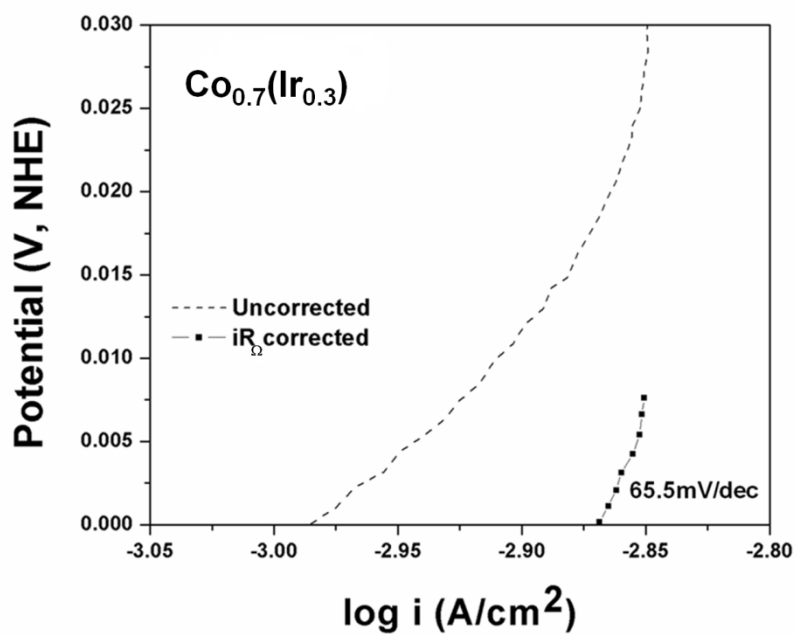


Figure S12: Tafel polarization plot of $\text{Co}_{0.7}(\text{Ir}_{0.3})$, before and after iR_{Ω} correction.

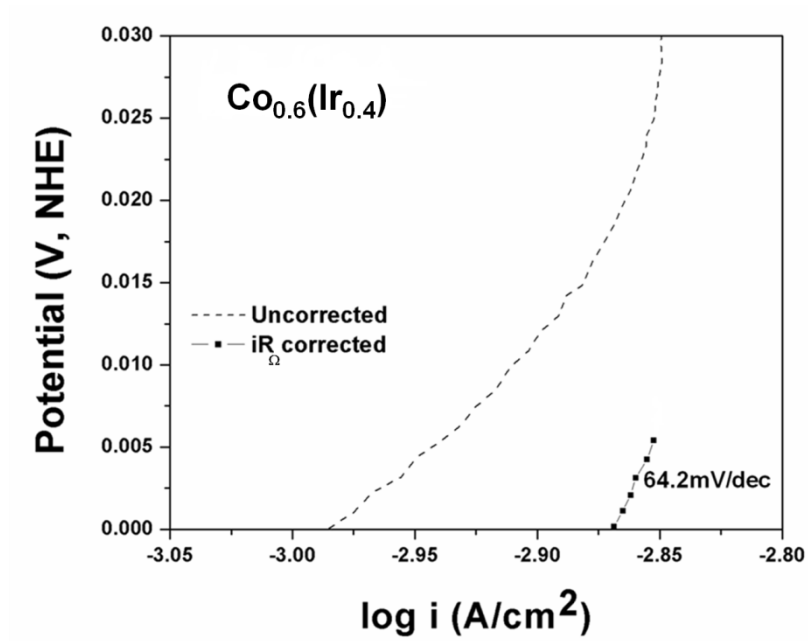


Figure S13: Tafel polarization plot of $\text{Co}_{0.6}\text{Ir}_{0.4}$, before and after iR_{Ω} correction.

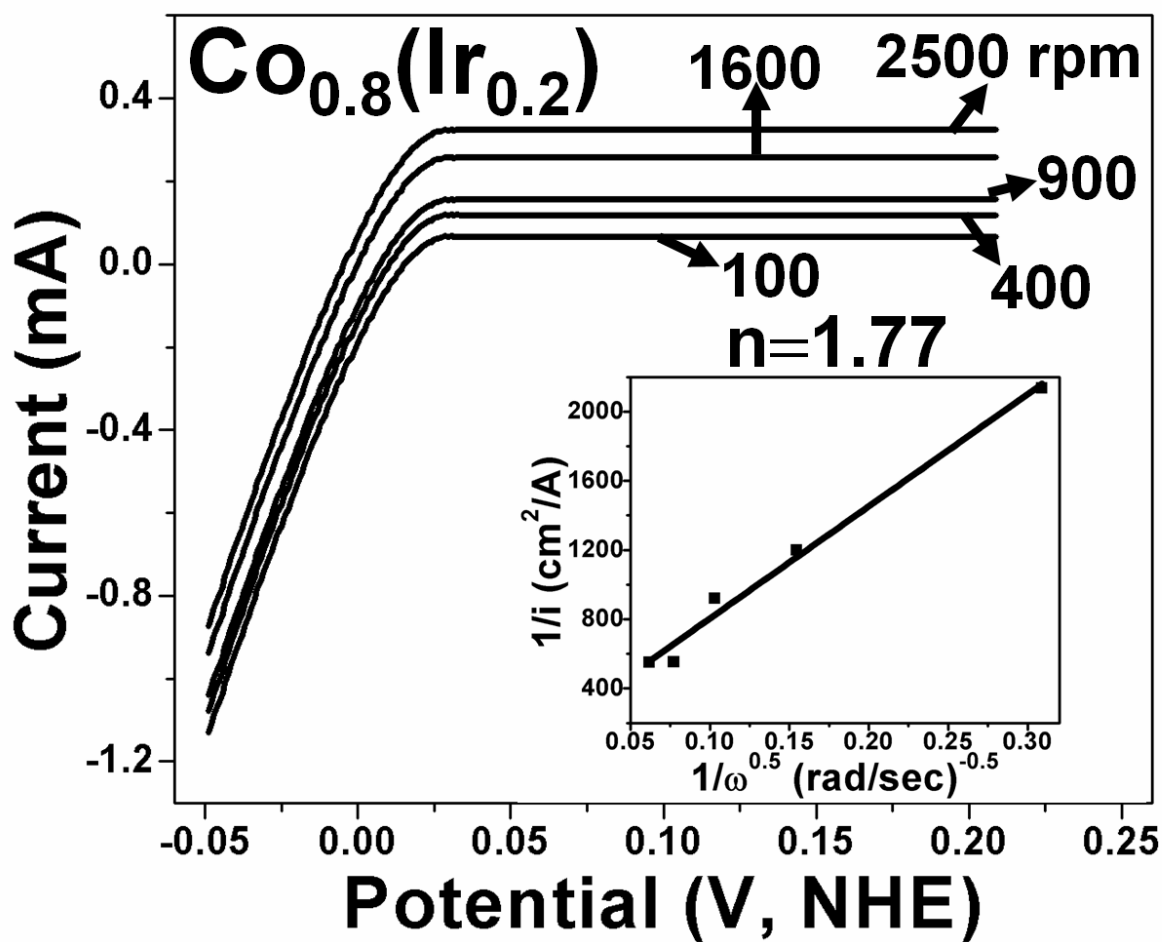


Figure S14: The polarization curve for HOR of $\text{Co}_{0.8}\text{Ir}_{0.2}$ obtained on rotating disk electrode (RDE), measured in H_2 saturated 0.5 M H_2SO_4 electrolyte solution at 40°C with a scan rate of 10 mV/sec. Koutechy-Levich plot obtained for $\text{Co}_{0.8}\text{Ir}_{0.2}$ is shown in the inset of the polarization curve.

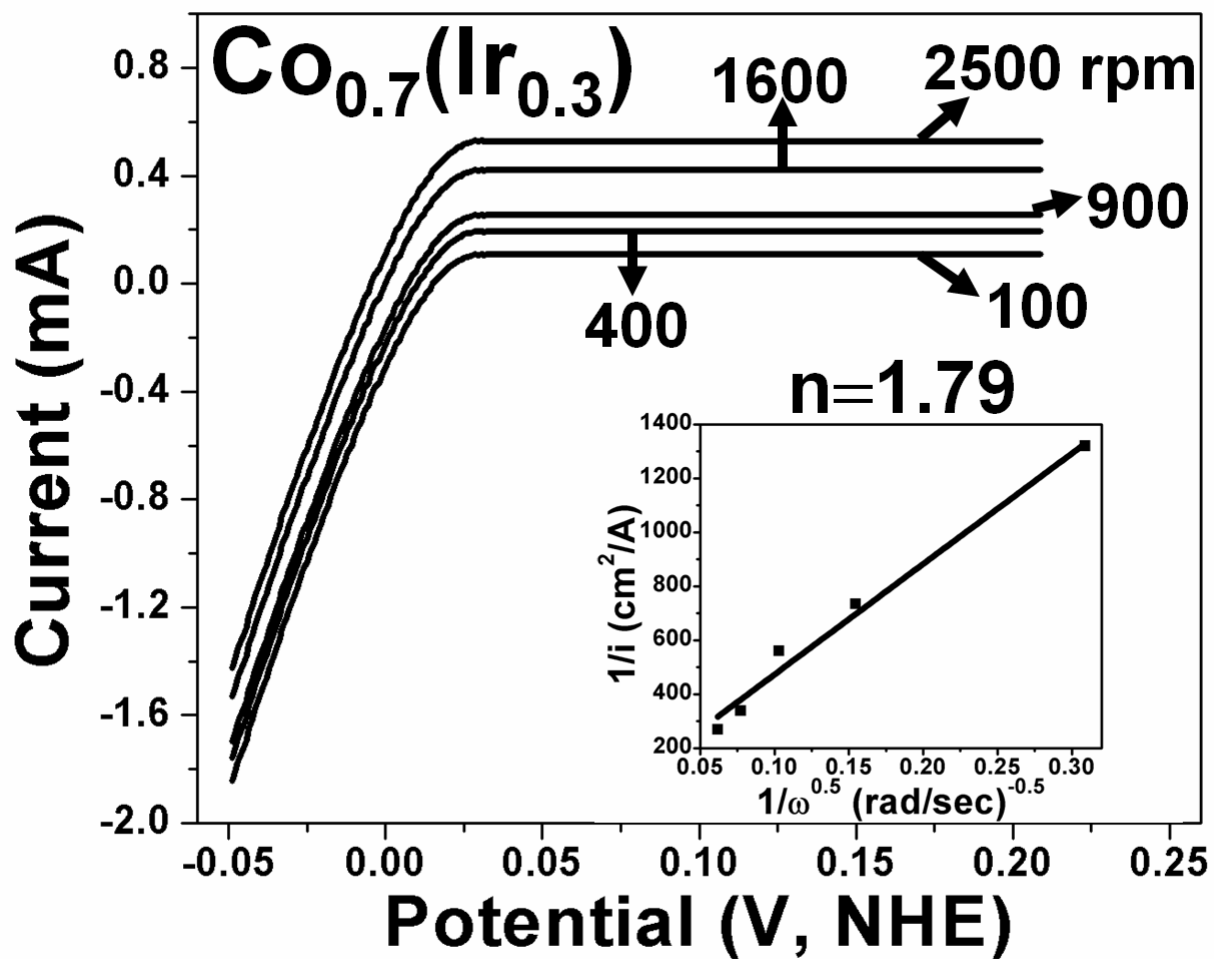


Figure S15: The polarization curve for HOR of $\text{Co}_{0.7}(\text{Ir}_{0.3})$ obtained on rotating disk electrode (RDE), measured in H_2 saturated 0.5 M H_2SO_4 electrolyte solution at 40°C with a scan rate of 10 mV/sec. Koutechy-Levich plot obtained for $\text{Co}_{0.7}(\text{Ir}_{0.3})$ is shown in the inset of the polarization curve.

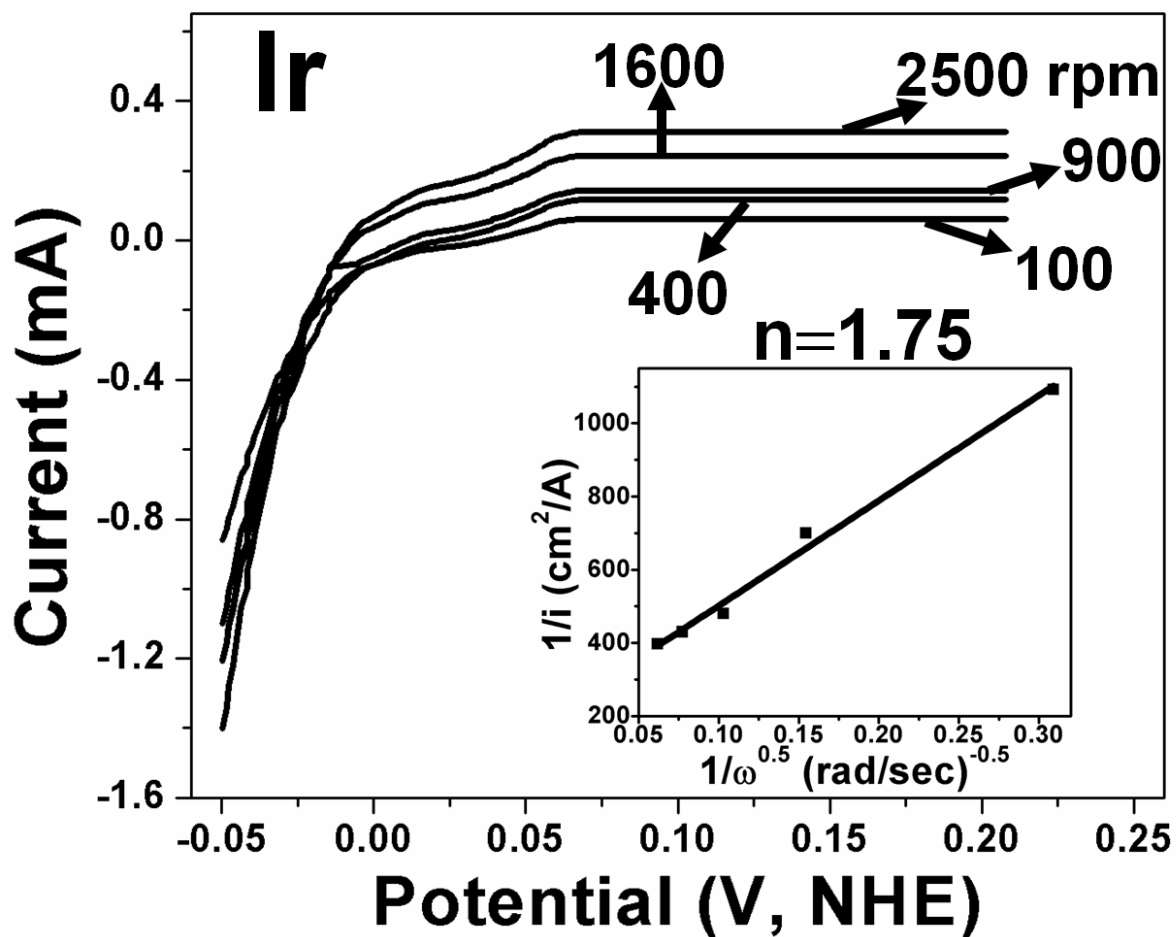


Figure S16: The polarization curve for HOR of Ir-NPs obtained on rotating disk electrode (RDE), measured in H_2 saturated $0.5 \text{ M H}_2\text{SO}_4$ electrolyte solution at 40°C with a scan rate of 10 mV/sec . Koutechy-Levich plot obtained for Ir is shown in the inset of the polarization curve.

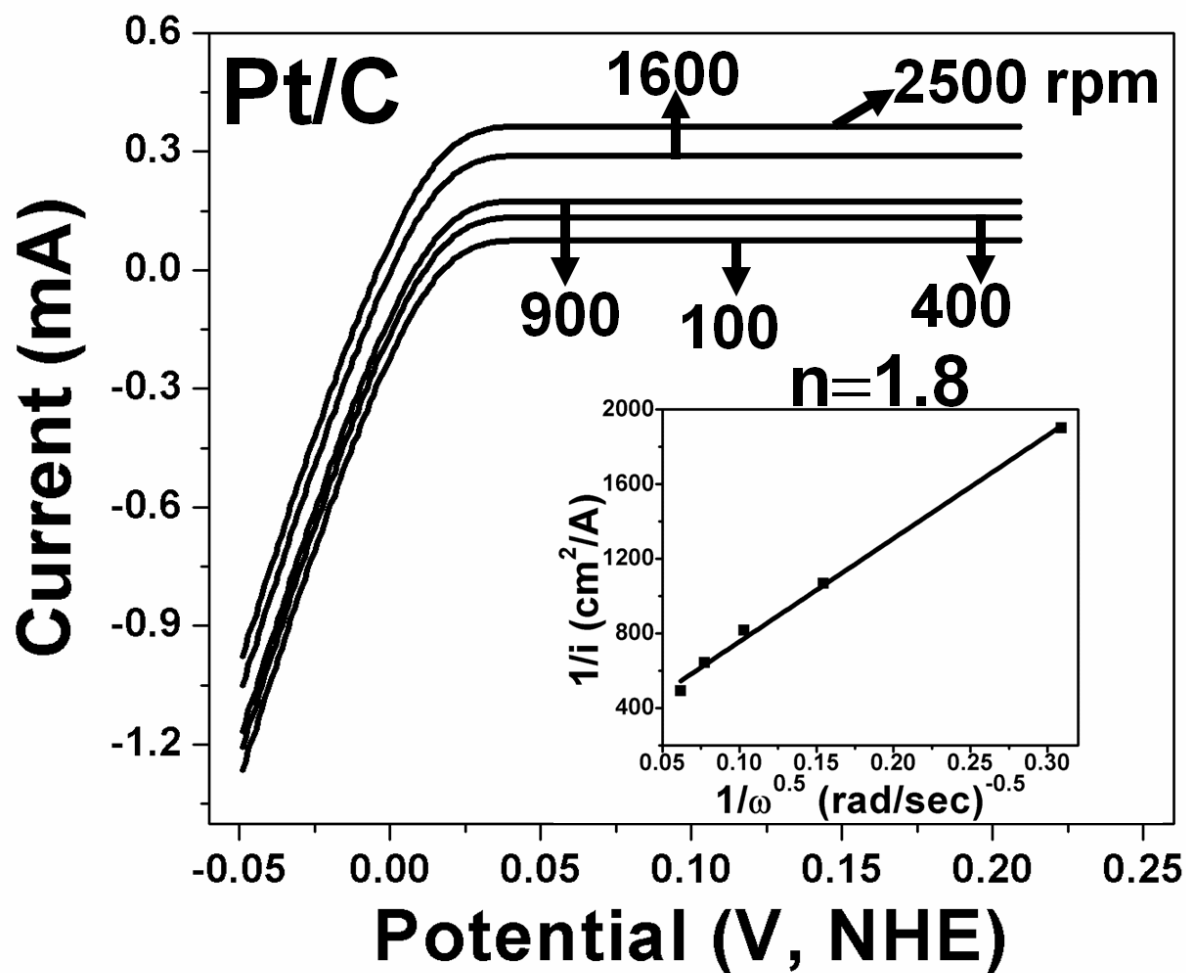


Figure S17: The polarization curve for HOR of Pt/C obtained on rotating disk electrode (RDE), measured in H_2 saturated 0.5 M H_2SO_4 electrolyte solution at 40°C with a scan rate of 10 mV/sec. Koutechy-Levich plot obtained for Pt/C is shown in the inset of the polarization curve.

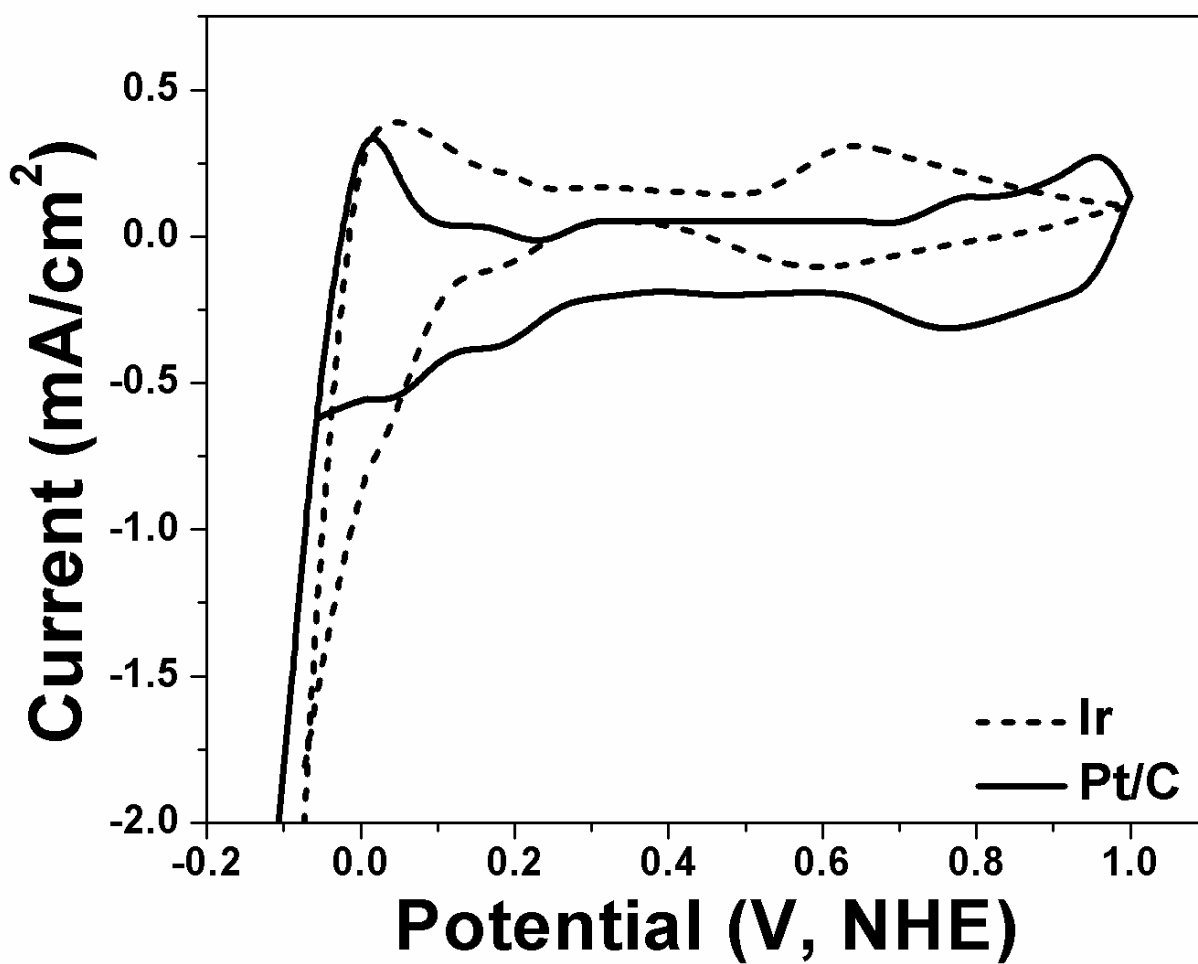


Figure S18: The cyclic voltammetry (CV) curve obtained for Ir-NPs and Pt/C, measured in N₂ saturated 0.5 M H₂SO₄ electrolyte solution at 40°C collected at a scan rate of 10 mV/sec.

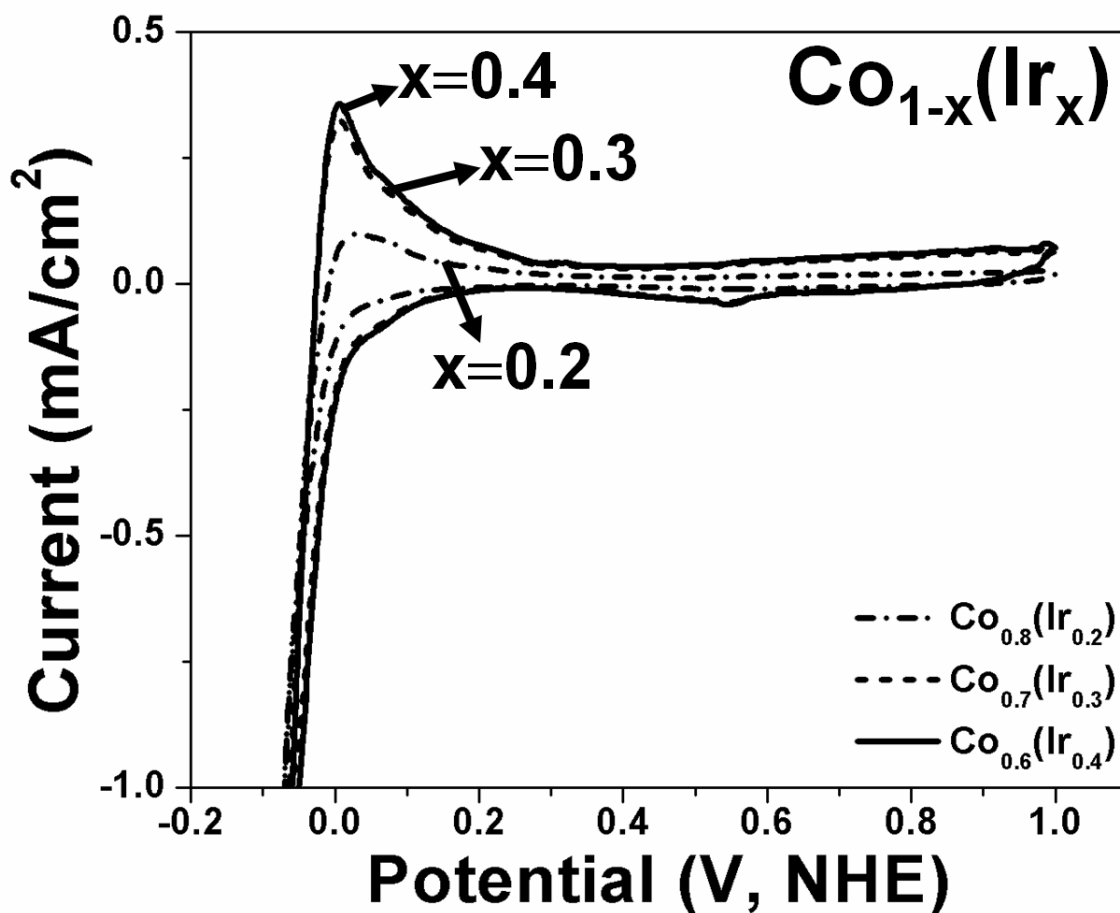


Figure S19: The cyclic voltammetry (CV) curve of Co_{1-x}(Ir_x) (x=0.2, 0.3, 0.4), measured in N₂ saturated 0.5 M H₂SO₄ electrolyte solution at 40°C at scan rate of 10 mV/sec.